CONF-951135--16
SAND95-1651C

NDI USING MM-WAVE RESONANT TECHNIQUES

J. S. Martens and S. Sachtjen
Conductus, Inc.

N. R. Sorensen
Sandia National Laboratories

ABSTRACT

Millimeter wave resonant measurements are commonly used for surface and near-surface materials characterization including the detection of cracks and defects, analysis of semiconducting and dielectric materials, and analysis of metallic electrical properties beneath coatings. Recent work has also shown the approach to be useful in evaluating corrosion products and the detection of incipient corrosion and corrosion cracking. In the analysis area, complex permittivity data of the corrosion products can be extracted, usually with accuracy of a few percent or better, to aid in identification of the product and possibly of mechanisms. In the detection area, corrosion-related cracks of order 100 μm or less near the surface have been detected and corrosion products have been detected beneath a variety of paints. Surface preparation requirements are minimal, particularly compared to some optical techniques, giving increased hope of field applicability. A number of examples of NDI on aircraft related materials and structures will be presented along with an assessment of detection and accuracy limits.

INTRODUCTION AND DESCRIPTION OF THE TECHNIQUE

Because of the increasing costs of aircraft maintenance and the radically increasing age of both military and civilian aircraft fleets, there is an obvious need for improved NDI techniques. One area of interest is that of incipient surface corrosion detection (beneath paint) and the early detection

DISTRIBUTION OF THIS DOCUMENT IS UNLIMITED

MASTER

DISCLAIMER

This report was prepared as an account of work sponsored by an agency of the United States Government. Neither the United States Government nor any agency thereof, nor any of their employees, make any warranty, express or implied, or assumes any legal liability or responsibility for the accuracy, completeness, or usefulness of any information, apparatus, product, or process disclosed, or represents that its use would not infringe privately owned rights. Reference herein to any specific commercial product, process, or service by trade name, trademark, manufacturer, or otherwise does not necessarily constitute or imply its endorsement, recommendation, or favoring by the United States Government or any agency thereof. The views and opinions of authors expressed herein do not necessarily state or reflect those of the United States Government or any agency thereof.

DISCLAIMER

Portions of this document may be illegible in electronic image products. Images are produced from the best available original document.

of corrosion-related cracking (e.g., near rivets). One class of technique that may be able to perform well in that area are based on resonant mm-wave analysis.

Microwave and mm-wave resonant techniques have been used for decades to extract properties of materials (e.g., [1]-[2]). The simplest conceptual approach is the box cavity shown in Fig. 1. Microwave energy is coupled in and out through a small aperture (not shown). When the frequency is such that a dimension of the cavity is an integral number of wavelengths (appropriately defined), reflections off the walls add in-phase creating a resonant condition. Because of the in-phase addition, any changes to the loss in the system (wall conductivity or loss in the inserted sample) are readily measurable. In addition, any dielectric present in the system alters the resonant frequency since the wave velocity in the dielectric is different from that in the rest of the cavity. Thus, dielectric properties can be extracted directly as well.

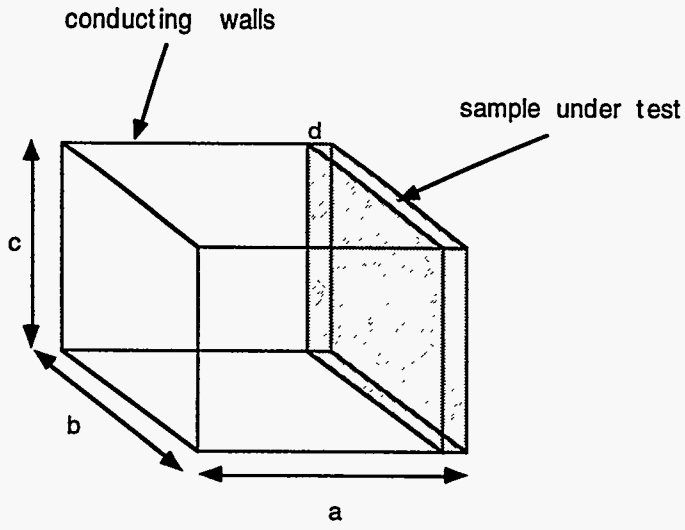

Figure 1. *A simple box cavity to illustrate the principles of high frequency materials measurements.*

While simple to picture, this cavity structure is not particularly practical because the sample would either have to be within the cavity or mounted flush to achieve uniform capacitive coupling around the edge. The difficulties with that approach in the context of aircraft parts are apparent. The confocal resonator approach (e.g., [3]-[4]), used in surface resistance analysis, on the other hand, is more amenable to these measurements. This quasi-optical structure (shown in Fig. 2) consists of a spherical mirror focusing the microwave/mm-wave radiation onto a small spot on the sample under test. The sample surface can be imaged by rastering the sample or the measurement

hardware, whichever is more convenient, allowing the detection of corrosion on various parts of a surface.

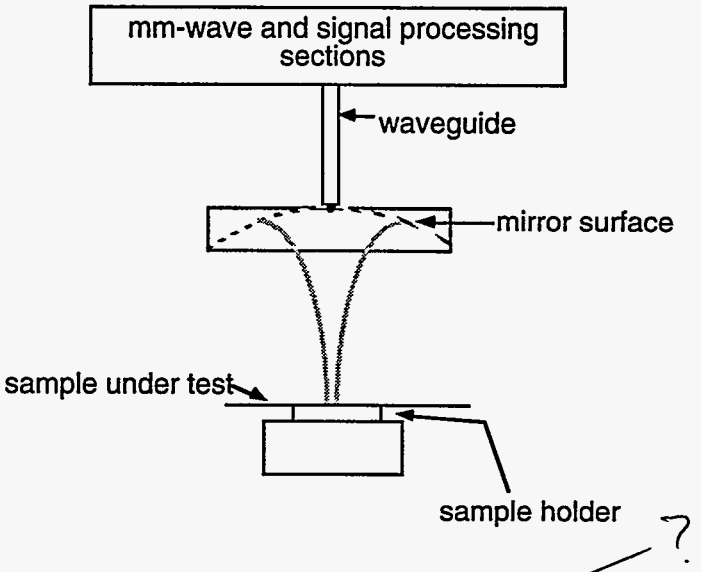

Figure 2. *The quasi-optical approach discussed in this proposal (surface resistance analysis or confocal resonator are other terms). The sample is not contacted and can be imaged in a reasonably accurate manner using this tool.*

Measurement speed is important, particularly in a high volume maintenance environment. At a single point, measurement time is much less than 1 second and scan times are generally only mechanically limited. As an example, if 200 mm coupons are being tested and 25 points are to be measured, the scan time will generally be less than two minutes. On a larger aircraft part where the machine is to be moved around, it may take 5-10 minutes to sufficiently sample a square foot area. These estimates are dependent on the sampling density required by the problem.

In the measurement, two quantities are directly measured: the quality factor Q and the resonant frequency f_0 which were in the 90-100 GHz range for the experiments discussed here. The resonant frequency can be placed almost anywhere in the mm-wave range by proper choice of cavity geometry. The specific frequency range chosen is a compromise between high lateral resolution (higher frequencies are better) and stability/economics (lower frequencies are better).

The quality factor is inversely related to the linewidth of the resonance and decreases when the losses become larger (either from substrate resistivity increasing or dielectric loss increasing). The physical meaning of the resonant frequency is clear from the previous discussion on the box

resonator. From these measured quantities, the surface resistance can be extracted from a simple formula [4]

$$R_s = \frac{\pi f_0 \mu_0 b}{2Q} - R_{sm}$$

where b is the radius of curvature of the mirror, μ_0 is the free space permeability ($4\pi\ 10^{-7}$ H/m) and R_{sm} is the mirror surface resistance in Ω. The surface resistance, R_s, is the variable used in many of the plots to follow and is a good measure of the overall loss in a composite sample. The surface resistance represents the difficulty in inducing rf currents on the surface of the sample. Any semiconducting or insulating corrosion products or cracks formed on the surface will radically affect the ability to generate these currents and will result in an increased surface resistance.

In many cases, it is of interest to relate the materials parameters of a coating (permittivity and permeability) to the surface impedance that would be measured. A simple two layer model will be assumed (a coating or product on a conductor). As discussed above, the resonant frequency shifts because of the presence of a layer of different wave velocity. Thus, the difference in resonant frequency (with and without the product layer) provides information on the layer's properties and thickness. This relation is expressed as [5]

$$t \propto \frac{\Delta f_0}{c/v_{ph} - 1}$$

where t is the product thickness, Δf_0 is the change in resonant frequency and v_{ph} is the phase velocity in the material (nominally $\mathrm{Re}(1/(\mu\varepsilon)^{1/2})$). This effect will be dominated by the real parts of permittivity and permeability under lower loss conditions. More generally, the complex composite surface impedance (composite since it includes the effect of the coating and the underlying conductor) can be expressed as [6]-[7]

$$Z_{s,comp} = \sqrt{\frac{\mu}{\varepsilon}} \frac{R_{s1}(1+j) + \sqrt{\frac{\mu}{\varepsilon}} \tanh\left(d\sqrt{-\omega^2\mu\varepsilon}\right)}{\sqrt{\frac{\mu}{\varepsilon}} + R_{s1}(1+j)\tanh\left(d\sqrt{-\omega^2\mu\varepsilon}\right)}$$

where R_{s1} is the surface resistance of the underlying conductor (normally a few hundred milliohms at 94 GHz for most metals), d is the coating thickness, and μ and ε are the permeability and permittivity of the coating/product (respectively). The imaginary part of $Z_{s,comp}$ is manifested in the measured resonant frequency, since changes here represent changes in the phase length of the cavity. The real part of $Z_{s,comp}$ is the composite surface resistance and is derived from the directly measured cavity Q. There are two things making this expression frequency dependent. The coating/product acts as a transformer in many cases so there will be some frequency dependence (in the tanh function) from changing electrical thickness of the coating. The material parameters μ and ε may also be frequency dependent. In most corrosion products studied to date, the material frequency dependence has been a relatively minor effect.

In the analysis of samples, the surface resistance and resonant frequency are normally measured as a function of position. The complex dielectric parameters can then be extracted as a function of position. The absolute values can give information about the corrosion products since they represent the deviations from the base metal. Loss tangent is often useful in assessing the purity of a product in the case of many oxide growths (on aluminum for example) while the real part of permittivity can often give more compositional information (separating CuS from Cu_2S as an example). The variation of these properties with position can be interesting in itself. Changes in the variation of corrosion product properties can give some insight into nucleation changes and substantial deviations in surface resistance can be used to locate corrosion-induced defects. The examples in the rest of this document illustrate how the extraction of these properties can be used to investigate the corrosion and corrosion state of a variety of materials and structures relevant to aircraft NDI.

Al SALT FOG EXPOSURE

This set of samples consisted of coupons from 4 aluminum alloys (1100,2024,6061, and 7075) to be measured before and after salt fog exposure (168 hours, 3.5% solution of NaCl in water atomized). The object was to correlate the surface impedance/permittivity signatures extracted from the resonant technique with microscopic analysis.

Before exposure, the surface resistances of the alloys were all reasonably consistent with what one would expect for these bulk metals with some starting surface oxide. Starting samples with varying levels of oxides affected the absolute numbers but not the relative changes to any great

degree. After exposure, the surface impedance changed dramatically as indicated in the table below. Here W=windward and L=leeward refers to the side of the sample receiving and looking away from the salt fog generator respectively. The measured numbers are surface resistances in ohms.

Alloy	Before	After W	% change	After L	% change
1100	0.176	0.226	*+28%*	0.208	*+18%*
6061	0.222	0.305	*+37%*	0.266	*+20%*
7075	0.258	0.461	*+79%*	0.376	*+46%*

There is clearly a difference among the alloys in corrosion resistance, as has been confirmed by many other measurement techniques (quartz microbalance, microscopic inspection,...). The thickness of the corrosion products was extracted from resonant frequency differentials and the ratio of these thicknesses (1100 product thickness:6061 product thickness: 7075 product thickness) was about 1:2.2:4. Compared to an overage thickness assessment from profilometry, the extracted thicknesses were accurate to within about 5%. This is not necessarily a meaningful comparison since the thickness variations across the samples were substantial. The permittivities were reasonably stable (5% shifts) suggesting the bulk of the differences in surface resistance signature are due to impurity incorporation. Before and after contour maps of the 6061 alloy are shown in Fig. 3 to illustrate the fairly dramatic nature of the surface resistance shift.

DISCLAIMER

This report was prepared as an account of work sponsored by an agency of the United States Government. Neither the United States Government nor any agency thereof, nor any of their employees, makes any warranty, express or implied, or assumes any legal liability or responsibility for the accuracy, completeness, or usefulness of any information, apparatus, product, or process disclosed, or represents that its use would not infringe privately owned rights. Reference herein to any specific commercial product, process, or service by trade name, trademark, manufacturer, or otherwise does not necessarily constitute or imply its endorsement, recommendation, or favoring by the United States Government or any agency thereof. The views and opinions of authors expressed herein do not necessarily state or reflect those of the United States Government or any agency thereof.

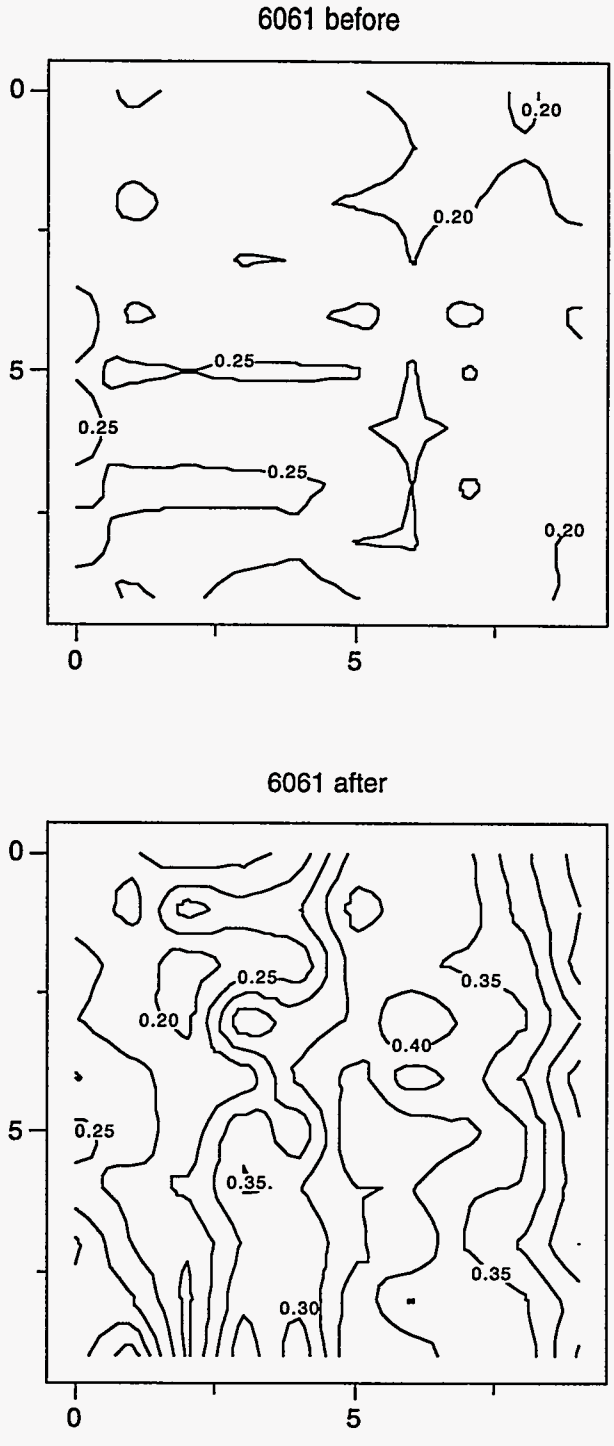

Figure 3. *Contour plots of a section of 6061 Al before and after salt fog exposure. The contour labels are surface resistances in ohms. The absolute change is obvious as is the increase in inhomogeneity. The lateral scales are 2 mm/div (full scale, the plots are 10 divisions wide).*

The loss tangent of the product layer also increases through the series of samples from about 0.005 to 0.015. The accuracy on the loss tangent extraction is again about 5% in this range but repeatable to within about 1%. Since the loss tangents are all higher than that of pure Al_2O_3, the product layers are becoming increasingly diverse chemically as one moves through the series with the 7075 product layer being dominated by contaminant oxides. This is also consistent with many microscopic observations. Also of interest is that the standard deviation of loss tangent (on a spatial basis) is about 8 times higher for the 7075 than for the 1100 suggesting a 7075 nucleation model with very different distance scales.

These observations would be consistent with nucleation centering on the denser impurity sites. Further evidence is provided by some limited multi-frequency analysis which showed the standard deviation of loss tangent decreasing away from the metal surface. The complex dielectric properties would be more unstable near these impurity sites and would presumably become somewhat more stable at the upper layers of the product.

SAMPLE WITH RIVET HOLES AND OTHER STRESSES

Since one of the critical corrosion problems involves subsurface cracking near rivet holes, samples to simulate this condition were generated (pending actual aircraft samples). Rivet holes were placed in a 7075 coupon (1/8" thick) that had already had salt fog exposure but was not coated with any pretreatment. The sample was then placed under bending stress while in a salt water environment (to accelerate any effects) for 24 hours. The before and after contour maps are shown in Fig. 4. Prior to the stress and exposure, the holes were clearly defined by deviations in local surface resistance. After exposure, another region of elevated surface resistance appeared around the hole areas that is asymmetric. Since the bending force was applied against the vertical edges of the image, this may be consistent with microcrack formation. A more complete analysis needs to be done of this type of test, but a change was detected around the holes that could not be detected optically.

what about bending with no salt water exposure?

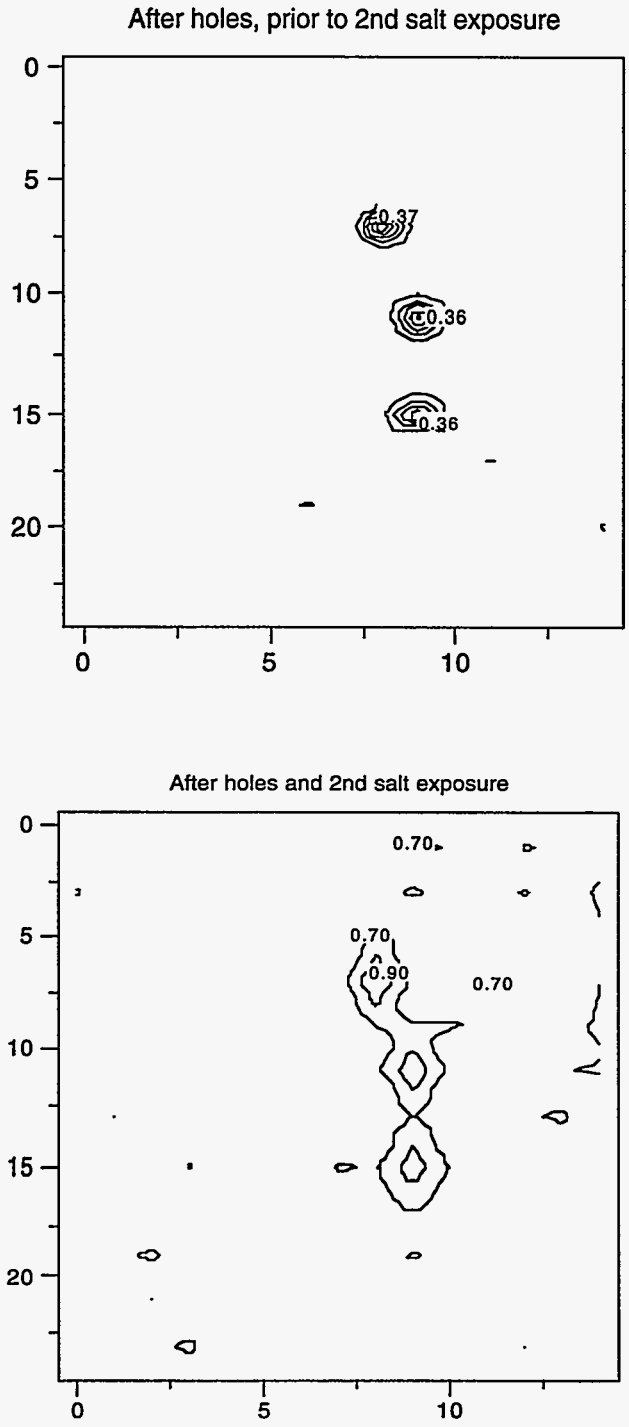

Figure 4. *Surface resistance contour plots (in ohms) of a 7075 coupon with rivet-like holes placed in it. The images are for before and after a salt exposure. Note the added elongated distortion in the surface resistance data after exposure. The contour values start at a high level to focus on the hole areas. The significant surface disruption of the corrosion on the blank metal is not shown.*

Some additional tests were conducted to try to correlate the surface resistance signature with the exposure conditions and, if possible, to the incipient crack sizes. A measure that was used was the effective area that had a surface resistance elevated at least 50% above the background mean. Since the rivet hole sizes were constant (diameter of about 5 mm), this should provide a measure of the disrupted area.

Because of time constraints, only a limited number of tests were run, but the data illustrates a clear trend. Keep in mind that the effective area includes the rivet hole itself. Small cracks were microscopically evident for the last row in the table with sizes on the order of 100 μm. This should give some estimate of the measurable effect size.

Conditions	**Effective elevated area (mm^2)**
1 day, nominal bending stress	76
2 days, nominal bending stress	81
3 days nominal bending stress	85
4 days, double bending stress	93

UNDERNEATH PAINT

Since in many field applications it would be desirable to detect corrosion beneath paint, it is important to determine if (a) paints are too lossy to allow this measurement and (b)what degree of sensitivity is possible. The first experiments were conducted with steel coupons painted with either epoxy or powder paints. A scratch of 1±0.2 mm width was cut in the paint and the coupons exposed to salt fog (at the site of a commercial customer). The final coupon was then measured to see if corrosion was detectable beneath the paint. Figure 6 shows the results for two coupons measured under these circumstances. The scratch extends horizontally from x=0 index marks to about x=10 in both cases. The background surface resistance stayed in the 0.3-0.4 ohm range but the disruption near the scratch is significant. In the heavy exposure case, disruption in surface resistance is visible nearly 2 cm from the scratch. Since the spot size is certainly no larger than 5 mm, this indicates the presence of products beneath the paint surface at a significant distance from

the scratch. The total disruption width is about 50 mm in the heavy case and 35 mm in the moderate case.

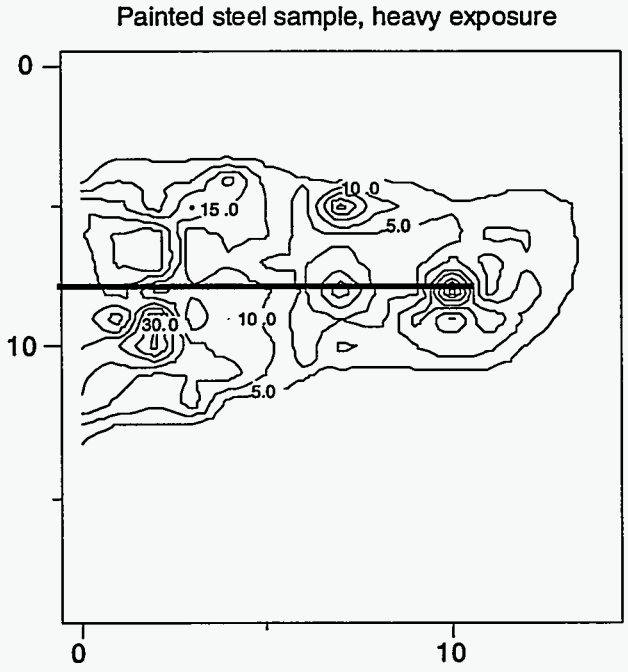

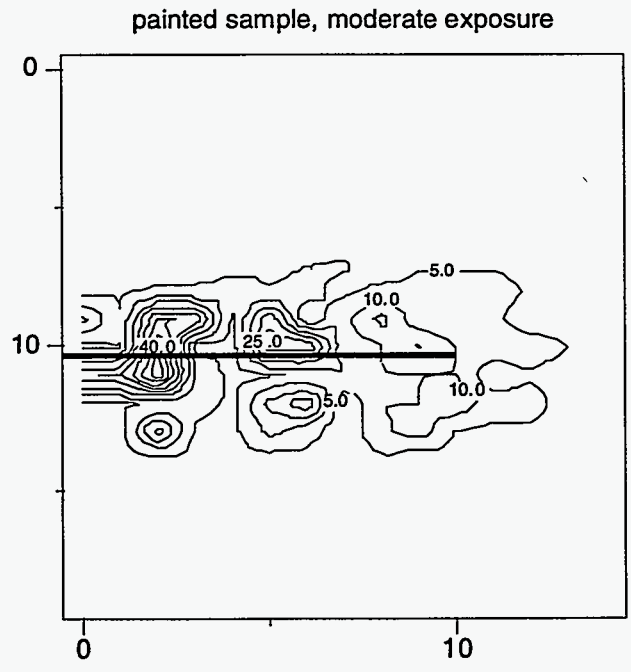

Figure 5. *Contour plot of painted steel sample (with a scratch 1 mm wide) exposed to a salt fog environment for two different durations. The lateral scales are 5 mm/div and the contour labels are surface resistances. The position of the scratch is indicated approximately by the heavy black line.*

The experiments were repeated on some aluminum samples and in no case was the paint loss a significant factor in corrosion detection. The disruption on surface resistance did not exceed 7% while the relative change in the corroded areas was easily 20-40% and sometimes by orders of magnitude as shown in Fig. 6. The paint clearly impedes extraction of the real part of permittivity since an additional phase delay source is present but it should be less of a problem in detectability. This ability is extremely important in field application, since bare surfaces will often not be available.

TITANIUM

An alloyed Ti sample was exposed to a heated saline environment as an initial test. While this test clearly does not mimic the actual environment an engine part would be subjected to, it can help establish a detectability limit for the analysis. The primary growth will probably be a contaminated oxide, which should be detectable as in the aluminum alloys, but layer growth may be slower. Before and after exposure contour maps are shown in Fig. 6.

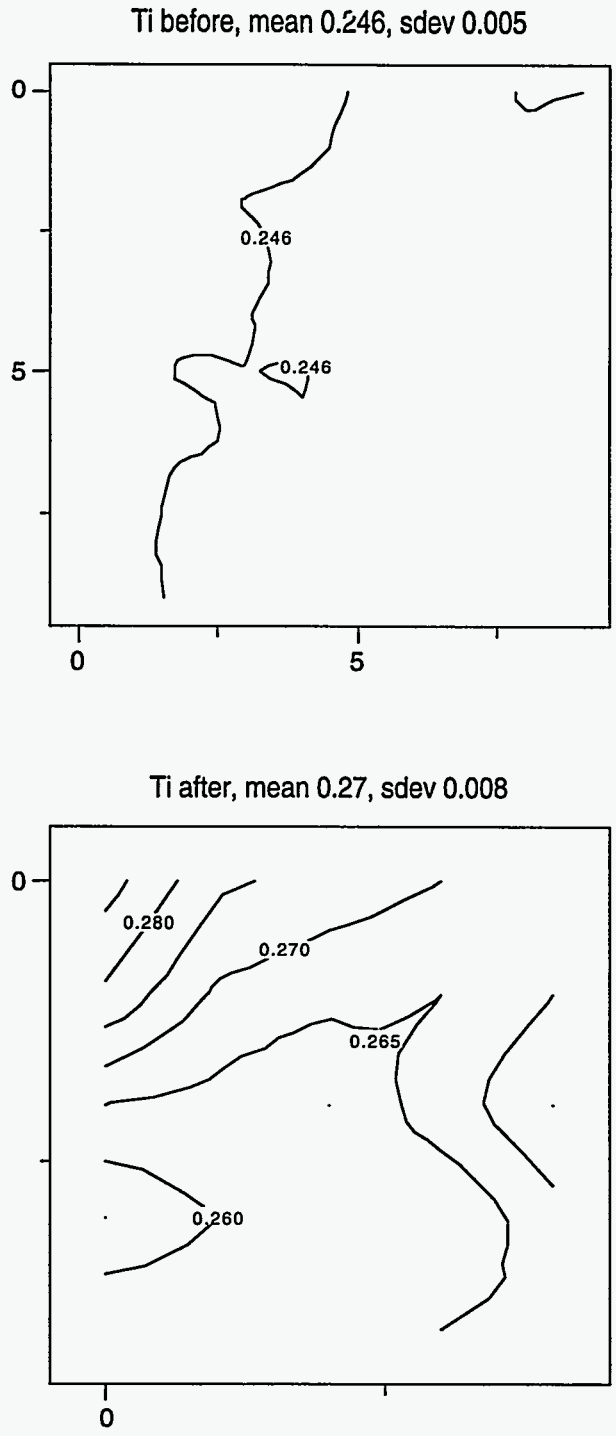

Figure 6. *Plot of a high temperature Ti sample before and after heated saline exposure. While more subtle than some of the other samples, the change in surface resistance is distinct and statistically significant.*

While more subtle, the changes here were detectable and were not visible with the unaided eye. The dielectric constant on the product material was approximately 20.5 with an uncertainty of about 5%. Since this is far below the value for TiO_2, it is likely the product is dominated by sub oxides or oxides with the impurities in the alloy. With additional experimentation, a better estimate of the composition of the oxide could be retrieved. The main purpose of this experiment was to confirm detectability in another important materials family.

CONCLUSIONS

A technique for corrosion detection and analysis based on mm-wave resonant surface resistance measurements has been presented. While the concept of high frequency cavity measurements for materials analysis is not new, this particular implementation and measurement sequence would appear to be more novel. The incipient detection (before optically observable) of Al, Ti and a steel example have all been discussed. The minimal detectable product thicknesses are all well below 100 nm (10 nm is probably a lower bound) with an accompanying set of data available of trends in both real and imaginary parts of the dielectric constant of the product. Incipient corrosion-related cracks around rivet holes have also been measured with features smaller than 100 μm being detectable. All of these analysis are based on the disruption in the ability to generate rf currents in the sample under test. The power levels are low, the measurements are fast, and the results repeatable to normally within 1% (in terms of surface resistance).

This work was supported in part by the Air Force Office of Scientific Research under SBIR contract No. F49620-94-C-0049.

This work was supported in part by the U.S. Department of Energy under contract number DE-AC04-94AL85000.

REFERENCES

[1] R. F. Harrington, Time Harmonic Electromagnetic Fields (McGraw-Hill, New York, 1961), chp. 7.

[2] A. R. von Hippel, ed., Dielectric Materials and Applications (MIT Press, Cambridge, 1954).

[3] G. D. Boyd and J. P. Gordon, "Confocal multimode resonator for millimeter through optical wavelength masers," Bell Sys. Tech. Jour., 40, 489 (1961).

[4] J. S. Martens, V. M. Hietala, D. S. Ginley, T. E. Zipperian and G. K. G. Hohenwarter, "Confocal resonators for measuring the surface resistance of high temperature superconducting films," Appl. Phys. Lett., 58, 2543 (1991).

[5] J. S. Martens, S. M. Garrison, and S. A. Sachtjen, Solid State Tech. **37**, no. 12, 51 (1994).

[6] J. S. Martens, D. S. Ginley, and N. R. Sorensen, "A novel millimeter-wave corrosion detection method," J. Electrochem. Soc. **139**, 2886 (1992).

[7] R. E. Collin, Foundations for microwave engineering (McGraw-Hill, New York, 1966), Chp. 5.